

PICTORIAL ESSAY

Magnetic Resonance Imaging of Non-ischemic Cardiomyopathies: A Pictorial Essay

Cristina I Olivas-Chacon, Carola Mullins, Kevan Stewart, Nassim Akle, Jesus E Calleros, Luis R Ramos-Duran

Department of Radiology, Texas Tech University Health Science Center El Paso, El Paso, Texas, USA

Address for correspondence:
 Dr. Cristina Ivette Olivas Chacon,
 Department of Radiology,
 4800 Alberta Avenue, El Paso,
 Texas - 79905, USA.
 E-mail: cristina.olivas@ttuhsc.edu



Received : 26-03-2015
 Accepted : 24-05-2015
 Published : 30-06-2015

ABSTRACT

Non-ischemic cardiomyopathies are defined as either primary or secondary diseases of the myocardium resulting in cardiac dysfunction. While primary cardiomyopathies are confined to the heart and can be genetic or acquired, secondary cardiomyopathies show involvement of the heart as a manifestation of an underlying systemic disease including metabolic, inflammatory, granulomatous, infectious, or autoimmune entities. Non-ischemic cardiomyopathies are currently classified as hypertrophic, dilated, restrictive, or unclassifiable, including left ventricular non-compaction. Cardiovascular Magnetic Resonance Imaging (CMRI) not only has the capability to assess cardiac morphology and function, but also the ability to detect edema, hemorrhage, fibrosis, and intramyocardial deposits, providing a valuable imaging tool in the characterization of non-ischemic cardiomyopathies. This pictorial essay shows some of the most important non-ischemic cardiomyopathies with an emphasis on magnetic resonance imaging features.

Key words: Cardiac, delayed gadolinium enhancement, non-ischemic cardiomyopathies, steady-state free precession

INTRODUCTION

Non-ischemic cardiomyopathies include chronic and progressive myocardial diseases, either primarily of the cardiac muscle or secondary to generalized systemic disorders leading to progressive adverse effects on the size, shape, and function of the cardiac muscle.^[1] Occasionally, patients are asymptomatic or have only minimal symptoms, but commonly present with signs of advanced stage heart

failure and dysrhythmias.^[2] Clinical management and prognosis depend on the etiology of the cardiomyopathy involved. Transthoracic ultrasound remains the major imaging tool in identifying anatomic and functional characteristics of the heart, allowing the classification of hypertrophic, dilated, or restrictive cardiomyopathy.

Cardiovascular Magnetic Resonance Imaging (CMRI) complements transthoracic ultrasound by allowing characterization of pathologic tissue and reliably assessing edema and fat infiltration using non-contrast T1- and

This is an open access article distributed under the terms of the Creative Commons Attribution-NonCommercial-ShareAlike 3.0 License, which allows others to remix, tweak, and build upon the work non-commercially, as long as the author is credited and the new creations are licensed under the identical terms.

For reprints contact: reprints@medknow.com

How to cite this article: Olivas-Chacon CI, Mullins C, Stewart K, Akle N, Calleros JE, Ramos-Duran LR. Magnetic Resonance Imaging of Non-ischemic Cardiomyopathies: A Pictorial Essay. J Clin Imaging Sci 2015;5:37. Available FREE in open access from: <http://www.clinicalimaging-science.org/text.asp?2015/5/1/37/159564>

Video available on www.clinicalimaging-science.org

Access this article online	
Quick Response Code:	Website: www.clinicalimaging-science.org
	DOI: 10.4103/2156-7514.159564

T2-weighted sequences. Phase-contrast techniques measure blood flow in concomitant valvular heart disease, and ischemia assessment can be performed with first-pass perfusion imaging during hyperemia.^[2]

Late gadolinium enhancement (LGE) techniques accurately image areas of myocardial fibrosis or infiltration.^[3] To perform LGE, a segmented gradient-recalled echo (GRE) sequence with an inversion pulse preparation is generally used. To obtain imaging of the entire heart (stack of short-axis slices), the acquisition is ECG gated, performed 10–15 min after bolus injection of 1 mmol/kg of gadolinium, and typically requires 10–12 breath-holds and a stable sinus rhythm. Gadolinium tends to accumulate in fibrotic regions of the myocardium, creating a hyperintense signal, which can be differentiated from normal myocardium after choosing a correct time of inversion (TI) to null the signal from normal viable myocardium. Since choosing the right TI can present a challenge, phase-sensitive inversion recovery (PSIR) can be used to alleviate the dependence on the TI value. Single-shot steady-state free precession (SSFP) sequences can be used to accelerate imaging for patients with arrhythmia or those unable to breath-hold with conventional protocols, but come with the cost of lower signal-to-noise ratio and spatial resolution.^[4] Table 1 summarizes the common sequences used in the evaluation of non-ischemic cardiomyopathies and their application.

Various enhancement patterns can be recognized using LGE. Subendocardial or transmural LGE located within the perfusion territory of an epicardial coronary artery can be classified as ischemic type, and abnormal enhancement not confined to a known vascular distribution is consistent with non-ischemic causes^[1] [Figure 1].

Subendocardial enhancement

Amyloidosis

Amyloidosis is a systemic glycoprotein deposition of misfolded proteins within the extracellular spaces

throughout the body. Cardiac involvement manifests as restrictive cardiomyopathy and is the cause of death in approximately half of the patients. On cine imaging, glycoprotein deposition results in biventricular myocardial thickening and restrictive cardiomyopathy resulting in as global hypokinesis [Video 1, Figure 2a and b]. Late fibrotic stages of restrictive cardiomyopathy secondary to amyloidosis can develop atrioventricular valvular abnormalities such as mitral and tricuspid insufficiency, which can be seen on cine imaging [Video 2].

Amyloid deposition within the heart results in the expansion of the extracellular space, allowing gadolinium-based contrast agents to be retained appearing as diffuse enhancement in the subendocardial region on LGE imaging^[5] [Figure 2c and d], which along with the abnormal gadolinium kinetics found in amyloidosis, makes choosing the right TI difficult. PSIR sequence can be helpful in these cases as it is independent of the TI value. In amyloidosis,

Table 1: Common sequences used in the evaluation of non-ischemic cardiomyopathies

Sequence name	Sequence usefulness
Cine SSFP	Myocardial structure and function
Cine fast gradient echo	Myocardial structure and function
T1-weighted black blood	Myocardial fat imaging
T2-weighted black blood	Tissue edema
Inversion recovery late enhancement	Late gadolinium enhancement
T2*	Myocardial iron content

SSFP: Single-shot steady-state free precession

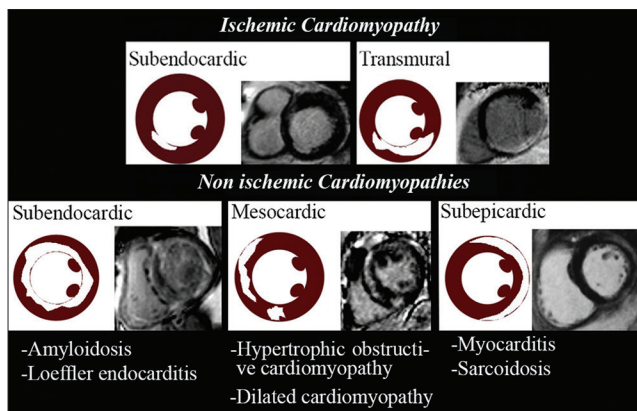


Figure 1: LGE patterns of ischemic and non-ischemic cardiomyopathies.

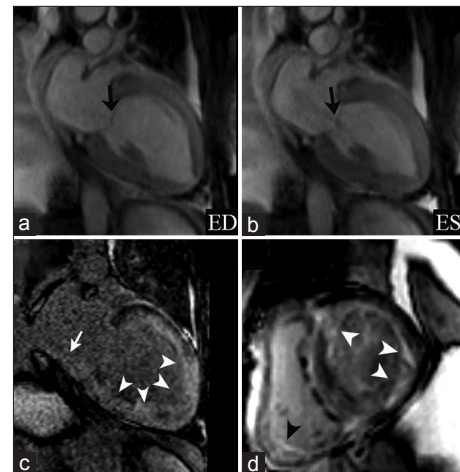


Figure 2: 60-year-old female with shortness of breath, diagnosed with systemic amyloidosis secondary to end-stage renal disease. 3 T CMRI gradient-recalled echo (GRE) cine images were taken to minimize the flow artifacts related to mitral insufficiency systolic jet. Two-chamber views (a and b) demonstrate myocardial wall thickening and global hypokinesis, along with a mitral insufficiency systolic jet (black arrows). Single-shot, phase-sensitive inversion recovery (PSIR) late gadolinium enhancement (LGE) with two-chamber (c) and short-axis (d) views show increased signal intensity diffusely distributed in the subendocardium, involving large areas of the left ventricle in a non-coronary artery distribution and also affecting the right ventricle (black arrowhead) and left atrium (white arrow). LGE is demonstrated transmurally involving the subepicardium at the apex and at the apical aspects of the anterior and inferior walls (white arrowheads). ED = End diastole, ES = End systole.

high myocardial uptake in addition to fast clearance and blood washout of intravenous administered gadolinium result in similar T1 values for blood and myocardium on cine imaging. Therefore, image acquisition should be performed shortly after contrast injection.^[5]

Loeffler endocarditis (hypereosinophilic syndrome)

Hypereosinophilic syndrome is a rare disorder characterized by eosinophilia with organ-system dysfunction caused by eosinophil-associated tissue damage. Cardiac involvement has traditionally been divided into three stages: Acute necrosis, thrombosis, and fibrosis. During the acute necrotic stage, patients are commonly asymptomatic, progressively presenting symptoms of restrictive cardiomyopathy

until the final fibrotic pathologic stage is reached due to scarring of the chordae tendinae and the endocardium is reached. Disruption of the anticoagulant endothelial lining along with blood stasis in areas of hypokinesis leads to thrombus formation within the endomyocardial surface [Figure 3a and b]. Thrombi found in Loeffler endocarditis differ from the thrombi found in apical myocardial infarction as they lack transmural enhancement with LGE, myocardial thinning, and perfusion defects in first-pass perfusion imaging in the subjacent myocardial wall [Video 3, Figure 3e].^[6,7] Using long inversion times (TI value > 422 ms), a thrombus can be differentiated from a tumor based on a characteristic pattern of hypointensity within its core.^[8]



Video 1: 48-year-old female with progressive dyspnea, diagnosed with light chain amyloidosis. 1.5 T CMRI single-shot steady-state free precession (SSFP) real-time cine imaging short-axis views from the mid-ventricle to the apex demonstrate myocardial wall thickening and global hypokinesis with a restrictive pattern indicating an underlying infiltrative cardiomyopathy.



Video 2: 60-year-old female with shortness of breath, diagnosed with systemic amyloidosis secondary to end-stage renal disease. 1.5 T CMRI gradient-recalled echo (GRE) cine imaging. Horizontal long-axis four-chamber view demonstrates myocardial wall thickening and global hypokinesis with a restrictive pattern. Two systolic jets are visualized through the mitral and tricuspid valves, consistent with mitral and tricuspid insufficiency due to infiltrative cardiomyopathy.

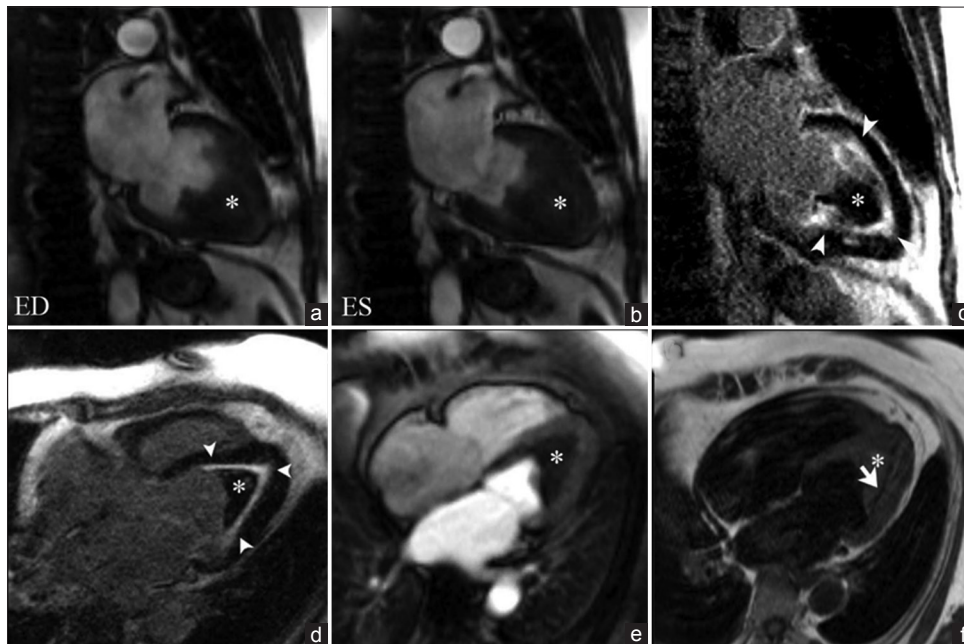


Figure 3: 45-year-old female with rapidly progressive congestive heart failure, diagnosed with Loeffler endocarditis. Steady-state free precession (SSFP) cine image (a and b) demonstrate an endocavitary filling defect in the apex of the left ventricle (asterisks). (c and d) Delayed enhancement inversion recovery (DEIR) images demonstrate a thin area of intense linear delayed enhancement (arrowheads) distributed along the apical endocardium of the left ventricle, subtending the distribution of the filling defect. (e) First-pass perfusion image shows a lack of gadolinium uptake consistent with a thrombus (asterisk). (f) T1-weighted Turbo Spin Echo (TSE) imaging shows the region of endocardial enhancement is markedly hypointense (white arrow), indicating dense subendocardial fibrosis. Note that the remainder of the myocardium deep to the subendocardial fibrosis shows normal signal intensity and perfusion. ED = End diastole, ES = End systole.



Video 3: 45-year-old female with rapid progressive congestive heart failure, diagnosed with Loeffler endocarditis. 1.5 T CMRI T1-weighted first-pass perfusion sequential imaging as gadolinium contrast transits through the heart at rest. An endocavitary filling defect lacking gadolinium uptake in the apex of the left ventricle is consistent with a thrombus. The remainder of the deep myocardium shows normal gadolinium uptake and perfusion.

On LGE imaging Loeffler endocarditis is characterized by an increased signal intensity within the subendocardial surface due to cell death and fibrosis. The distribution of the abnormal enhancement does not correspond to a vascular distribution [Figure 3c and d]. Late fibrotic stages produce a hypointense signal of the subendocardium on T1-weighted imaging [Figure 3f].

Subepicardial enhancement

Myocarditis

Myocarditis is an inflammatory disease of the myocardium with highly variable clinical manifestations ranging from subclinical disease to cardiogenic shock, arrhythmias, and sudden death. It can be caused by viral or bacterial infections, but also by drug toxicities and autoimmune disorders resulting in lymphocytic infiltrates as an interstitial inflammatory response.

On CMRI Inversion Recovery LGE, myocarditis is shown as predominant as a patchy subepicardial contrast enhancement in a non-vascular distribution [Figure 4a and c]. Increased signal intensity is seen in T2-weighted black-blood sequences due to myocardial edema matching the regions of abnormal enhancement as a marker of acute inflammation [Figure 4b and d].^[7]

Mesocardial enhancement

Dilated cardiomyopathy

Primary dilated cardiomyopathy is defined as left or biventricular dilatation with severely impaired systolic function with low ejection fraction, which can be either idiopathic or caused by non-ischemic insults including previous myocarditis, drug side effects, or alcohol abuse.

Impaired systolic function is observed on cine imaging as marked left ventricular (LV) dilation with global hypokinesis [Video 4, Figure 5], which may be accompanied by atrioventricular valve abnormalities, such

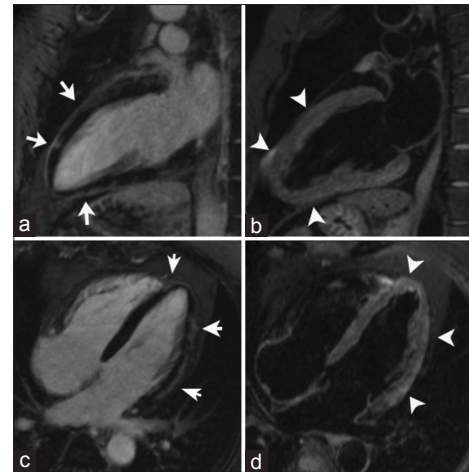


Figure 4: 43-year-old male with chest pain, diagnosed with post-streptococcal myocarditis. DEIR imaging with two chamber (a) and four chamber (c) views demonstrate patchy areas of myocardial enhancement following a subepicardial distribution (arrows) indicative of inflammatory tissue damage. T2-weighted black-blood images (b and d) demonstrate myocardial edema matching the regions of abnormal enhancement (arrowheads).

as mitral regurgitation related to outstretching of the valve annulus. Dilated cardiomyopathy shows an LGE pattern of mesocardial striae in the interventricular septum, along with enhancement of the right ventricle–left ventricle insertion points [Figure 6], secondary areas of replacement fibrosis and related to subclinical foci of myocardial ischemia that has been associated with electrical instability and the risk of sudden cardiac death.^[2,7]

Hypertrophic cardiomyopathy

Hypertrophic obstructive cardiomyopathy (HOCM) is the most frequent genetic cardiac disease. Affected individuals demonstrate myocyte hypertrophy, disarray, and fibrosis, presenting clinically as sudden death or heart failure.^[9] On CMRI cine imaging, significantly increased septal thickness during systole is demonstrated in a patient with asymmetric septal hypertrophy [Video 5]. With LGE imaging, a patchy, mid-myocardial hyperenhancement in the basal and mid-ventricular septum indicates myocardial fibrosis secondary to an insufficient blood supply to the hypertrophied myocardium [Figure 7]. The presence and extent of LGE has a prognostic value in the risk stratification of HOCM patients due to its correlation with ventricular arrhythmias and sudden cardiac death.^[2]

LV outflow tract obstruction is present in approximately 25% of HOCM patients. Mechanical impedance to outflow in HOCM typically occurs at the subaortic level, owing to mitral valve systolic anterior motion and mid-systolic contact with a hypertrophied ventricular septum. Severe LV outflow tract obstruction is defined as pressure gradient of > 50 mm Hg.^[10] In symptomatic individuals with a resting

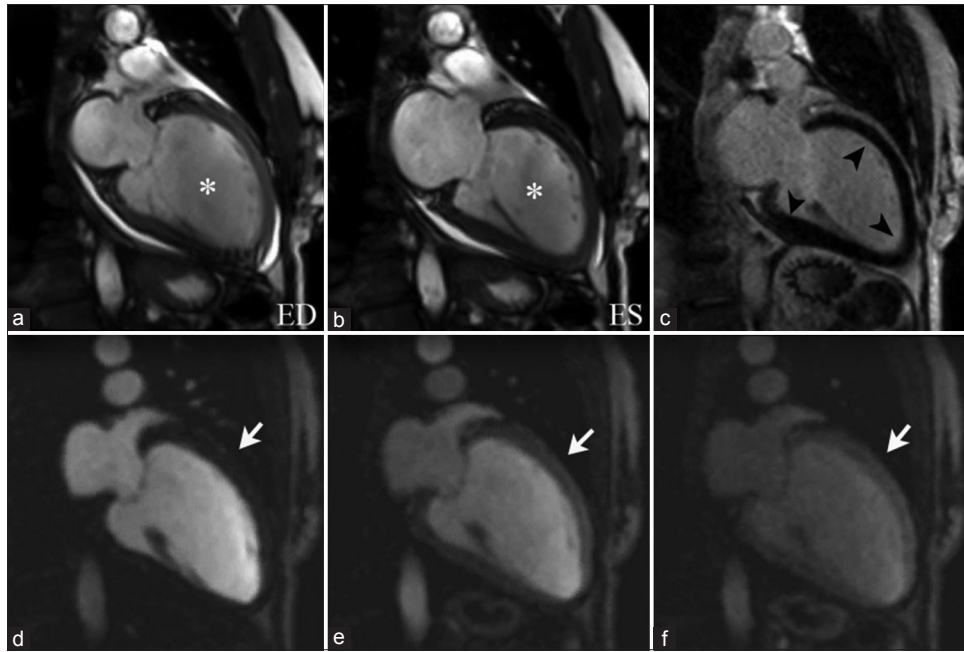


Figure 5: 72-year-old female with symptoms of congestive heart failure, diagnosed with dilated cardiomyopathy. SSFP imaging with two-chamber views at end diastole (a) and end systole (b) illustrate left ventricular dilation and global hypokinesis (asterisks). DEIR imaging (c) shows a fully viable myocardium without abnormal enhancement (arrowheads). Sequential imaging of first-pass perfusion (d–f) demonstrates no perfusion defects (arrows). These findings are consistent with non-ischemic dilated cardiomyopathy.

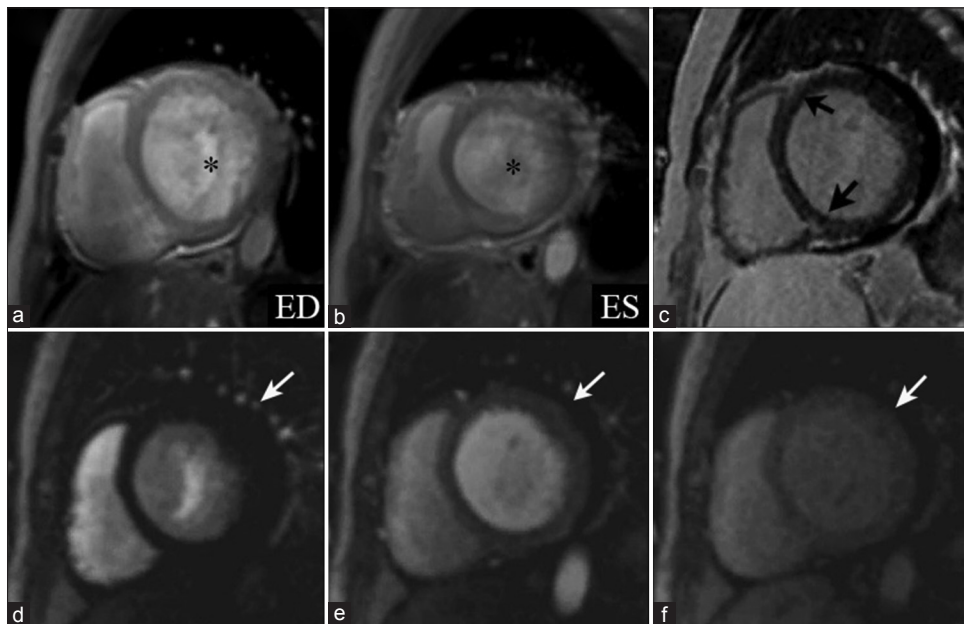


Figure 6: 53-year-old female with symptoms of progressive dyspnea, diagnosed with non-ischemic dilated cardiomyopathy. Short-axis views GRE imaging at end diastole (a) and end systole (b) demonstrate marked left ventricle dilation with global hypokinesis (asterisks). DEIR imaging (c) illustrates abnormal enhancement near the right ventricle–left ventricle insertion points (black arrows). Sequential first-pass perfusion imaging (d–f) demonstrate no perfusion defects within the myocardial wall (white arrows).

gradient of <30 mm Hg, hemodynamic obstruction can be provoked either through exercise or via Valsalva maneuver and visualized through echocardiography to explore management decisions.^[11]

With SSFP cine images, a flow jet at the level of the left ventricular outflow tract (LVOT) during systole

characterizes the presence of subaortic stenosis, which can be quantified using velocity-encoded mapping cine images [Figure 8].

If conservative treatment options have been exhausted, left ventricle outflow tract obstruction can be reduced by alcohol septal ablation or surgical procedures. Alcohol

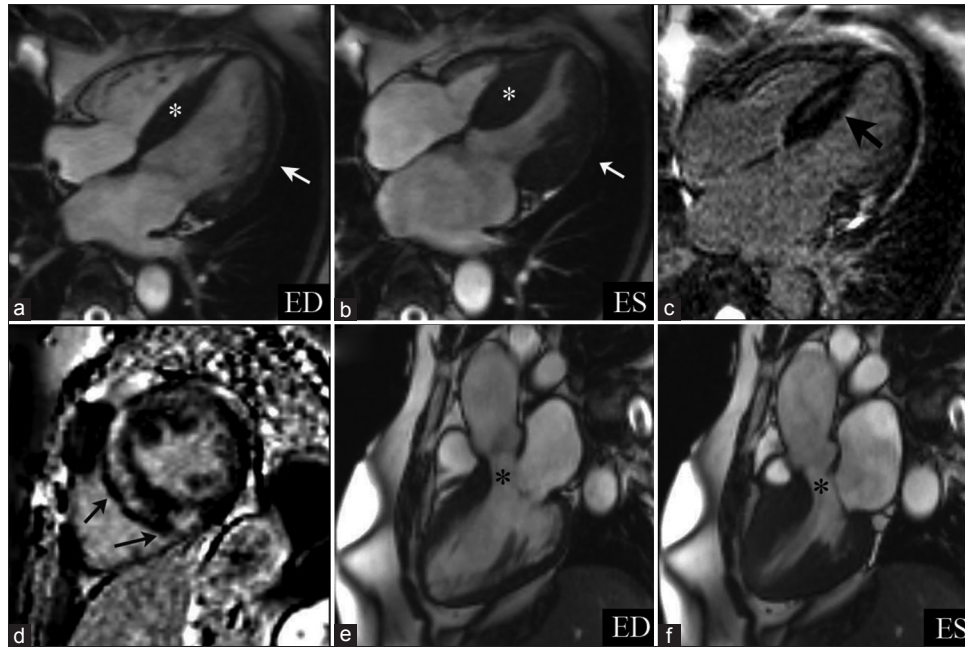


Figure 7: 35-year-old female with symptoms of progressive dyspnea, diagnosed with asymmetric hypertrophic cardiomyopathy. SSFP imaging at end diastole (a) and end systole (b) demonstrate a significantly thickened interventricular septum (white asterisks) and left ventricular lateral wall (white arrows). Phase sensitive inversion recovery single shot views (c and d) demonstrate a patchy, mid-myocardial hyperenhancement in the interventricular septum (black arrows) as a marker of myocardial fibrosis. SSFP three-chamber views at end diastole (e) and end systole (f) show no significant obstruction of the left ventricle outflow tract (black asterisks).



Video 4: 72-year-old female with symptoms of congestive heart failure, diagnosed with non-ischemic dilated cardiomyopathy. 3 T CMRI SSFP cine imaging with horizontal long-axis two- (left) and four-chamber (right) views illustrate left ventricular dilation and global hypokinesis.



Video 5: 35-year-old female with symptoms of progressive dyspnea, diagnosed with asymmetric hypertrophic cardiomyopathy. 1.5 T SSFP cine imaging demonstrates asymmetric septal systolic thickening.

septal ablation induces a partially controlled infarct of the basal septum with resultant scar formation and left ventricular (LV) remodeling. Following alcohol septal ablation, myocardial necrosis, edema, and microvascular obstruction can be depicted within the ablated myocardium on CMRI using perfusion imaging, SSFP steady-state free-precession, and post-gadolinium sequences.^[12]

Constrictive pericarditis

Constrictive pericarditis is the result of scarring and loss of the normal elasticity of the pericardial sac due to any cause of pericarditis. It is characterized by a thickened, fibrotic, and/or calcified pericardium, impairing cardiac filling leading to equalization of end-diastolic pressures in all four cardiac chambers. Patients with pericardial

constriction present with clinical manifestations of elevated systemic venous pressure and low cardiac output.^[13]

On cine imaging, generalized diffuse thickening of the pericardium can be observed, over the left side of the heart [Video 6], with an abnormal paradoxical motion of the interventricular septum during diastole exacerbated by inspiration which is known as septal bounce [Video 7, Figure 9]. The underlying cardiac cavities constricted by the abnormal pericardium have a flattened or tubular appearance. Increased ventricular filling pressures results in enlargement of the right atrium. Pericardial effusion with residual inflammation shows increased signal intensity on T2-weighted imaging, and can be further evaluated using T1 and T2 weighted sequences [Figure 10].

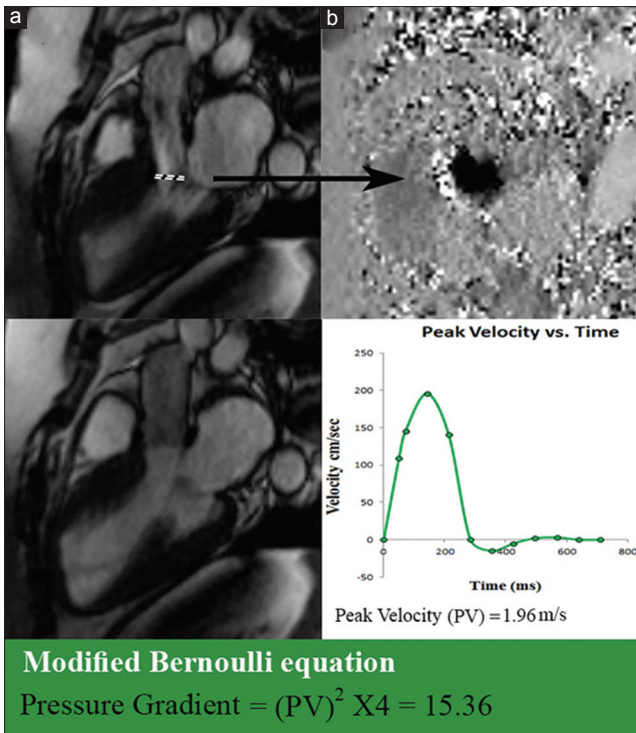


Figure 8: 21-year-old female with a family history of sudden cardiac death diagnosed with HOCM and mild subaortic stenosis. (a) SSFP cine imaging at mid systole at the level of the left ventricle outflow tract demonstrates a flow jet during systole (dashed line). (b) Phase velocity mapping aligned axially to the plane of the jet is used to obtain peak velocity (PV) flow through the narrowed LVOT. Using PV and the modified Bernoulli equation pressure gradient (15.36 in this patient) across, the LVOT narrowing is quantified.



Video 6: 53-year-old female with symptoms of cardiogenic shock, diagnosed with constrictive pericarditis. 3 T CMRI SSFP cine imaging with horizontal long-axis two-chamber (left) and four-chamber (right) views shows generalized diffuse thickening of the pericardium with posterior accentuation, tubular configuration of the ventricles, and right atrial enlargement along with paradoxical septal movement during systole.

LGE is useful in differentiating ongoing pericardial inflammation from pericardial fibrosis. Abnormal pericardial LGE is more frequently associated with histological findings of pericardial inflammation, including increased neovascularization, fibroblast proliferation, and granulation tissue. In contrast, patients without pericardial LGE are more likely to exhibit minimal neovascularization and mild or absent inflammation.^[14]

Myocardial non-compaction

Myocardial non-compaction is a rare entity that arises from

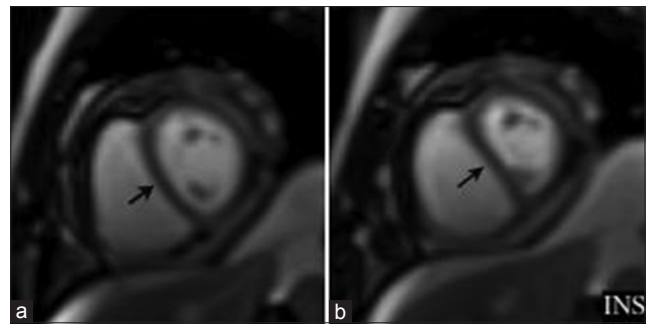


Figure 9: Cardiac MRI short-axis view single-shot SSFP free breathing imaging demonstrates paradoxical movement of the interventricular septum accentuated during inspiration (arrows). INS = inspiration.



Video 7: 3 T CMRI single-shot SSFP real-time cine imaging basal short-axis view during inspiratory maneuvers demonstrates paradoxical movement of the interventricular septum.

failure of compaction of the subendocardial myocardium and manifests as heart failure, arrhythmia, and systemic thromboembolic disease. The ventricle comprises two myocardial layers: The compact myocardium and the trabecular myocardium. Myocardial non-compaction usually affects the left ventricle, but can also show biventricular or isolated right ventricle involvement in rare cases.^[15] Distribution of LV segments with non-compaction can vary from one patient to another, but it often involves the apical, mid-inferior, and mid-lateral myocardial segments.^[16]

A commonly used diagnostic criterion is the ratio of the thickness of the trabeculated layer to the thickness of the compacted layer (T/C). To identify left ventricular non-compaction echocardiography requires the T/C to be >2.0 at end systole and >2.3 at end diastole in CMRI using the short-axis plane.^[17] The apex is commonly excluded due to its very thin myocardium.^[18]

On cine imaging [Video 8, Figure 11], prominent LV trabeculations with deep intertrabecular recesses are indicative of diffuse non-compacted areas in the mid-ventricular and apical LV wall, along with marked LV dilation and global hypokinesia.

The described macroscopic LGE patterns in LVNC are non-specific, including subendocardial, intramyocardial and transmural enhancement patterns.^[19]

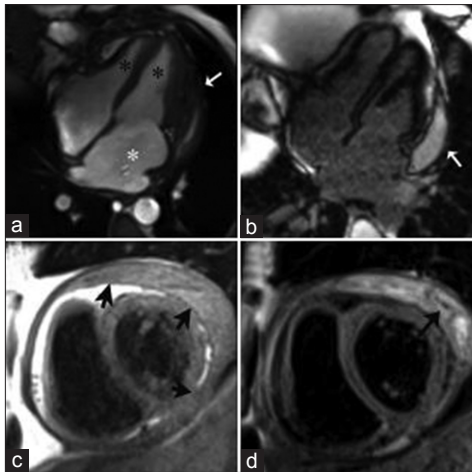


Figure 10: 53-year-old female with symptoms of cardiogenic shock, diagnosed with constrictive pericarditis. SSFP imaging at mid-diastole (a) shows generalized diffuse thickening of the pericardium with posterior accentuation (white arrow), tubular configuration of the ventricles (black asterisks), and right atrial enlargement (white asterisk). DEIR imaging (b) shows a posterior pericardial effusion (white arrow). TSE T1-weighted imaging (c) shows significant diffuse pericardial thickening (black arrows). TSE T2-weighted imaging with fat saturation (d) demonstrates the loculated and septated nature of the complex effusion (black arrow).

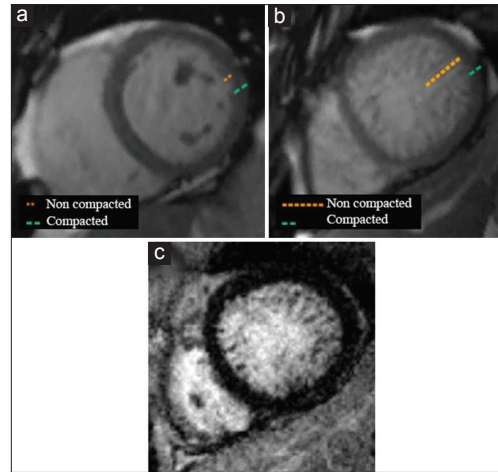


Figure 11: Comparison of (a) normal myocardial compaction of an asymptomatic 58-year-old female with (b and c) a 53-year-old female with progressive dyspnea diagnosed with myocardial non-compaction. (b) SSFP imaging demonstrates a diffusely thickened and hypertrabeculated non-compacted layer of the myocardium at the left mid-ventricle, more accentuated in the lateral wall. (c) As illustrated by DEIR, no abnormal areas of hyperenhancement are seen.

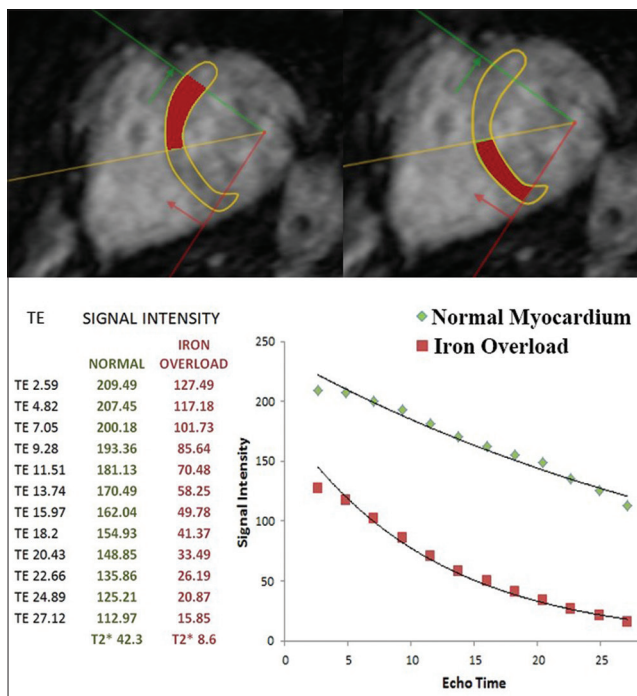


Figure 12: Graphic representation of T2* darkening in the heart. Average signal intensity (arbitrary units) is plotted as function of echo time (milliseconds). Representative signal intensity of two hearts are shown at increasing echo times (TE) from 2.59 to 27.12 ms. Heart 1 (green) has normal iron levels, remains with high signal intensity, and shows a shallow decay curve, whereas heart 2 with iron overload (brown) shows a more rapid decay curve.

The prominent myocardial trabeculae and deep recesses found in LVNC lead to a stagnant blood flow, resulting in the formation of clots in the left ventricle and thromboembolic events in 21–38% of all patients.^[20]



Video 8: 53-year-old female with progressive dyspnea, diagnosed with myocardial non-compaction. 3 T CMRI mid-ventricular short-axis views with SSFP cine imaging (upper row) demonstrate dilated and hypokinetic left ventricle with extensive areas of non-compacted myocardium, more accentuated in the lateral wall. Delayed enhancement inversion recovery (DEIR) imaging (lower row) shows no abnormal areas of hyperenhancement.

Myocardial iron overload

Systemic iron overload due to hemosiderosis and transfusion-dependent anemias can lead to cardiac involvement with dilated or restrictive cardiomyopathy. Iron chelation therapy is guided by CMR T2* relaxometry. CMRI detects iron indirectly. The paramagnetic effects of stored iron in the form of ferritin and hemosiderin cause signal loss in the affected tissues. Iron deposits cause surrounding water protons to lose phase coherence and local irregularities in the magnetic field leading to signal loss and shorter relaxation times on T1, T2, and T2* sequences. Times represent higher myocardial iron content and more advanced disease.^[21] Iron overload in the heart is “defined” as an RT2* <20 ms.^[22] Single short-axis views are used for myocardial T2* measurements, as shown in Figure 12.

CONCLUSION

Non-ischemic cardiomyopathy is a group of heterogeneous diseases. Determining the particular cause requires clinical correlation and often myocardial biopsy. Through a wide range of sequences, CMRI offers a unique non-invasive tool that allows *in vivo* tissue characterization distinguishing edema from fat, fibrosis, and myocardial infiltration. CMRI allows quantification of functional impairment and differentiates ischemic from non-ischemic caused based on various enhancement patterns. Therefore CMRI is an excellent complementary imaging tool in assessing the morphologic and functional characteristics of various cardiomyopathies.

Financial support and sponsorship

Nil.

Conflicts of interest

There are no conflicts of interest.

REFERENCES

- Mahrholdt H, Wagner A, Judd RM, Sechtem U, Kim RJ. Delayed enhancement cardiovascular magnetic resonance assessment of non-ischaemic cardiomyopathies. *Eur Heart J* 2005;26:1461-74.
- Kassi M, Nabi F. Role of cardiac MRI in the assessment of nonischemic cardiomyopathies. *Methodist Debaque Cardiovas J* 2013;9:149-55.
- Bluemke DA. MRI of nonischemic cardiomyopathy. *AJR Am J Roentgenol* 2010;195:935-40.
- Ferreira PF, Gatehouse PD, Mohiaddin RH, Firmin DN. Cardiovascular magnetic resonance artefacts. *J Cardiovasc Magn Reson* 2013;15:41.
- Maceira AM, Joshi J, Prasad SK, Moon JC, Perugini E, Harding I, et al. Cardiovascular magnetic resonance in cardiac amyloidosis. *Circulation* 2005;111:186-93.
- Ogbogu PU, Rosing DR, Horne MK 3rd. Cardiovascular manifestations of hypereosinophilic syndromes. *Immunol Allergy Clin North Am* 2007;27:457-75.
- Cummings KW, Bhalla S, Javidan-Nejad C, Bierhals AJ, Gutierrez FR, Woodard PK. A pattern-based approach to assessment of delayed enhancement in nonischemic cardiomyopathy at MR imaging. *Radiographics* 2009;29:89-103.
- Pazos-López P, Pozo E, Siqueira ME, García-Lunar I, Cham M, Jacobi A, et al. Value of CMR for the differential diagnosis of cardiac masses. *JACC Cardiovasc Imaging* 2014;7:896-905.
- Maron BK, Ommen SR, Semsarian C, Spirito P, Olivetto I, Maron MS. Hypertrophic cardiomyopathy: Present and future, with translation into contemporary cardiovascular medicine. *J Am Coll Cardiol* 2014;64:83-99.
- Geske JB, Cullen MW, Sorajja P, Ommen SR, Nishimura RA. Assessment of left ventricular outflow gradient: Hypertrophic cardiomyopathy versus aortic valvular stenosis. *JACC Cardiovasc Interv* 2012;5:675-81.
- Afonso LC, Bernal J, Bax JJ, Abraham TP. Echocardiography in hypertrophic cardiomyopathy The role of conventional and emerging technologies. *JACC Cardiovasc Imaging* 2008;1:787-800.
- Knight CJ. Alcohol septal ablation for obstructive hypertrophic cardiomyopathy. *Heart* 2006;92:1339-44.
- Bogaert J, Francone M. Cardiovascular magnetic resonance in pericardial diseases. *J Cardiovasc Magn Reson* 2009;11:14.
- Zurick AO, Bolen MA, Kwon DH, Tan CD, Popovic ZB, Rajeswaran J, et al. Pericardial delayed hyperenhancement with CMR imaging in patients with constrictive pericarditis undergoing surgical pericardiectomy: A case series with histopathological correlation. *JACC Cardiovasc Imaging* 2011;4:1180-91.
- Gomathi SB, Makadia N, Ajit SM. An unusual case of isolated non-compacted right ventricular myocardium. *Eur J Echocardiogr* 2008;9:424-5.
- Jenni R, Oechslin E, Schneider J, Attenhofer Jost C, Kaufmann PA. Echocardiographic and pathoanatomical characteristics of isolated left ventricular non-compaction: A step towards classification as a distinct cardiomyopathy. *Heart* 2001;86:666-71.
- McNally EM, Patel AR. Cardiac magnetic resonance of left ventricular trabeculation: The new normal. *Circ Cardiovasc Imaging* 2011;4:84-6.
- Dawson DK, Maceira AM, Raj VJ, Graham C, Pennell DJ, Kilner PJ. Regional thicknesses and thickening of compacted and trabeculated myocardial layers of the normal left ventricle studied by cardiovascular magnetic resonance. *Circ Cardiovasc Imaging* 2011;4:139-46.
- Grothoff M, Pachowsky M, Hoffmann J, Posch M, Klaassen S, Lehmkuhl L, et al. Value of cardiovascular MR in diagnosing left ventricular non-compaction cardiomyopathy and in discriminating between other cardiomyopathies. *Eur Radiol* 2012;22:2699-709.
- Cevik C, Shah N, Wilson JM, Stainback RF. Multiple left ventricular thrombi in a patient with left ventricular noncompaction. *Tex Heart Inst J* 2012;39:550-3.
- Kondur AK, Li T, Vaitkevicius P, Afonso L. Quantification of myocardial iron overload by cardiovascular magnetic resonance imaging T2* and review of the literature. *Clin Cardiol* 2007;32:E55-9.
- Pennell DJ. T2* Magnetic Resonance: Iron and Gold. *J Am Coll Cardiol Img* 2008;1:579-81.